ACS OMEGA

http://pubs.acs.org/journal/acsodf
Article

Coal Structure Characteristics of the 2# Coal Seam in the Jiaozuo Mining Area and Its Geological Dependence

Hongyue Duan, Yulong Ma, Jiyao Wang,* Yinlong Lu, and Weidong Xie*

Cite This: *ACS Omega* 2023, 8, 39242−39249

ABSTRACT: To clarify the coal structure, spatial distribution, and controlling factors of the 2# coal seam in Jiaozuo mining, the drilling coal samples were collected to observe the coal type and coal structure. The coal macerals were identified by a MPVSP microscope photometer, and the spatial characteristics of the coal structure were obtained through interpreting deep lateral resistivity logging, natural gamma ray logging, density logging, and acoustic logging curves. The influence of coal properties, burial depth, geological stress, and faults on the coal structure were discussed correspondingly. The results exhibit that granulitic−mylonite coal was most developed in the 2# coal seam, followed by primary coal and cataclastic coal; the coal type was dominated by semibright coal, followed by clarain and semidull coal. Granulitic−mylonite, cataclastic, and primary coals were the main components of clarain, semibright coal, and semidull coal, respectively. Higher vitrinite and organic matter contents were conducive to the development of granulitic−mylonite. The coal structure combinations were spatially varied, and the granulitic−mylonite combinations were the most common. Granulitic−mylonite coal was developed in the east and south parts of the study area, and the coal structure was fragmented with a greater burial depth and larger thickness. The geological stress is the fundamental cause of coal structure damage as well as the cutting of faults.

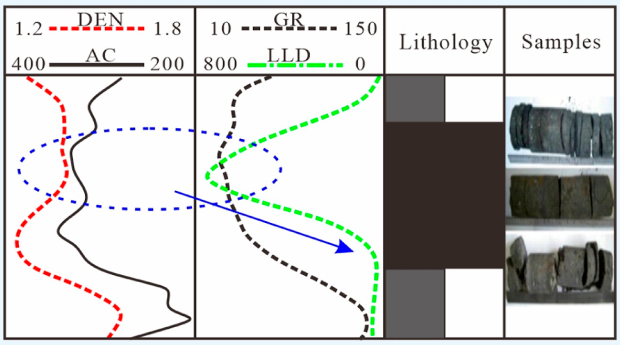

1. INTRODUCTION

The coal structure is a significant basis for the design of coal seam mining, which also has an important impact on the porosity and permeability of coal reservoirs.[1,2] Hence, it is necessary to clarify the coal structure characteristics before the exploitation of the coal seam and coalbed methane. Coal structure refers to the structural characteristics of coal seams that have undergone various geological processes, and it is categorized into primary coal, cataclastic coal, granulitic coal, and mylonite coal with a gradually fragmented structure.[3,4] Coal sample observation and logging curve interpretation are the common methods to clarify the vertical coal structure characteristics and their combinations, as well as the spatial variation in different areas.[5,6] The observation of coal samples includes the coal type, coal structure, and maceral. The deep lateral resistivity logging (LLD), gamma ray logging (GR), density logging (DEN), and acoustic logging (AC) logging curves are widely used in the exploration of coal fields, and the coal structure can be identified according to the amplitude, amplitude variation, shape, and peak of these curves.[7,8] The coal structure is influenced by coal spatial distribution, properties, and geological conditions.[9,10] The maturity of coal increases with greater burial depth, resulting in variations in molecular component, molecular structure, pore structure, hardness, density, and ductility.[11,12]

Additionally, the thickness of the coal seam also has an impact on the coal structure. There is also a specific relationship between the coal type and the coal structure. Primary coal is mainly found in semidull coal as well as some semibright coal. Cataclastic coal is mostly developed from semibright coal, followed by semidull coal and clarain. Granulitic coal and mylonite coal are generally found in clarain, as well as some semibright coal, while it is rare in semiduall coal.[5,13] The influence of geological conditions is mainly reflected in the differences in geological stress, which include maximum horizontal stress, minimum horizontal stress, vertical stress, and horizontal stress difference.[14,15] All of these stresses would destroy the primary structure of coal.[14,15] The geological structures of faults and folds also influence the coal structure significantly, especially the former.[16,17] The cutting effect of faults on the strata seriously damages its integrity, leading to the fragmentation of coal seams.[16,17]

Received: June 29, 2023
Accepted: September 27, 2023
Published: October 10, 2023

https://doi.org/10.1021/acsomega.3c04643
ACS Omega 2023, 8, 39242−39249

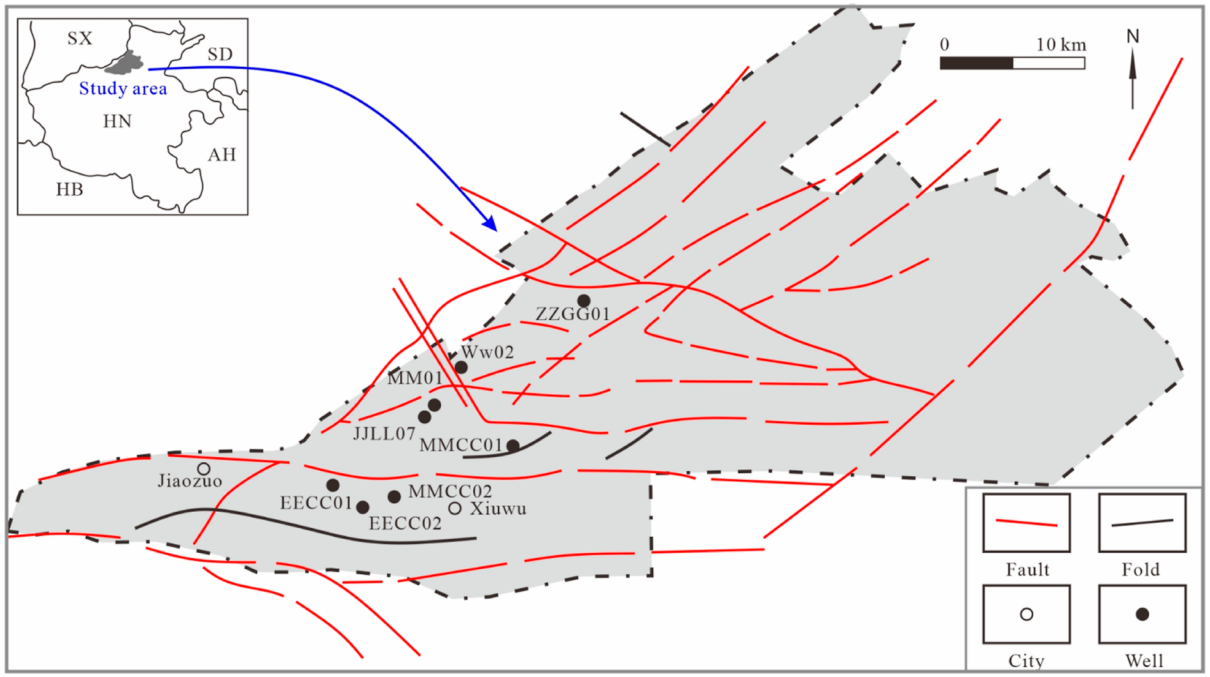

Figure 1. Location and structure outline of the Jiaozuo mining area.

Table 1. Logging Curve Characteristics of Different Coal Structures[a]

type of coal structure	primary coal	cataclastic coal	granulitic−mylonite coal
LLD	high amplitude, steep shape, and smooth peak	the amplitude is lower than that of primary coal and is in a stepped shape	low amplitude, and in a stepped, convex, or box shape
GR	low amplitude, in a flat or wavy shape	the amplitude is slightly higher than that of primary coal	the amplitude variation is not obvious
AC	high amplitude, and the peak is generally in a gentle, wavy shape	the amplitude is slightly higher than primary coal	the amplitude is higher than the former two, and the peak is in an irregular or wavy shape
DEN	high amplitude without significant variation	the amplitude is slightly lower than primary coal	the amplitude decreases significantly, and most of them are in large, wavy shapes

[a]Notes: DEN, GR, AC, and LLD are density, natural gamma ray, acoustic, and deep lateral resistivity logging curves, respectively.

Owing to the characteristics of high gas content, low pressure, and high coal and gas outburst risk, the Jiaozuo mining area was chosen as the research object of this work. The main mining 2# coal seam has undergone multiple stages of tectonic movements on different scales in the Mesozoic and Cenozoic eras since its formation.[18] It is generally suggested that the more severe the structural damage to the coal, the lower the strength of the coal, the more structural fractures there are, and the greater the outburst risk correspondingly.[5,19] Multiple sets of coal seams are developed in the study area, with a complex coal structure and varying degrees of coal damage. Jiaozuo mining area has experienced multiple rounds of geological exploration and exploitation, and a large amount of geological data has been collected. Nevertheless, there is also a lack of targeted research on coal structure characteristics, its spatial distribution, and controlling factors. Therefore, to ensure the safe mining of the coal seam and provide a reference for the exploration and development of coalbed methane, the main mining 2# coal seam is selected as the research object. A total of 56 drilling core samples are collected from ten wells, and the coal type and coal structure of these samples are identified. A MPVSP microscope photometer is utilized to observe and calculate the maceral of coal samples, and the correlation between it and coal structure is discussed. Moreover, the DEN, GR, AC, and LLD logging curves are used to analyze the spatial characteristics of the coal structure. Finally, the influence of coal properties, burial depth, thickness of coal, geological stress, and faults on the coal structure are discussed correspondingly.

2. GEOLOGICAL BACKGROUND AND METHODS

2.1. Geological Background. Jiaozuo mining area is located at the southeast edge of the Taihang uplift zone, North China plate (Figure 1). It is generally a NE−SW trending monocline, dipping to SE, and the dip angle is mainly in the range of 10−25°. Faults are developed in the study area, dominating the high-angle normal faults. According to the strike of faults, they can be categorized into three groups, i.e., the NE direction (including the NNE direction), the nearly EW direction, and the NW direction. The NE direction faults are the most developed, which indicates that the Yanshanian movement laid the tectonic foundation.[18] Additionally, some wide and gentle folds are found in the southern part of the study area. The spatial distribution characteristics of the strata and the boundaries of the mine field are mainly controlled by the distribution of faults.

Thirteen to 15 layers' coal seam were recognized in the Carboniferous to Permian in the study area, in which the 2# coal seam in the Shanxi formation of the Lower Permian has a

https://doi.org/10.1021/acsomega.3c04643
ACS Omega 2023, 8, 39242−39249

large thickness and stable distribution, enabling it to be the main mining coal seam. Its burial depth is mainly in the range of 408.64 to 1156.28 m (658.71 m on average), with the characteristic of being deep in the southeast and shallow in the northwest. The vitrinite reflectance ranges from 3.34 to 4.78%, which is at the stage of anthracite.[19] The coal seam is extremely sensitive to stress and strain, and its physical structure, chemical structure, and optical characteristics change significantly after being transformed by tectonic stress. 2# coal seam underwent multiple stages of tectonic transformation, mainly including the Hercynian, Indosinian, Yanshanian, and Himalayan movements. Consequently, primary coal is gradually transformed into cataclastic coal, granulitic coal, and mylonite. Due to the differences in the intensity of tectonic movements, the coal structure of the 2# coal seam in the study area also exhibits strong heterogeneity characteristics.

2.2. Sample Collection and Experiments. A total of 56 drilling core samples were collected from ten wells, and coal type, coal structure, and macroscopic fracture observations were conducted on these samples. Subsequently, the coal maceral tests were performed by using a MPVSP microscope photometer. In this experiment, samples were ground into particles with a size of less than 1 mm. Then, the particles were mixed with the binder in a 2:1 ratio, and the mixed samples were heated and compacted into coal bricks. Prior to observation, a side of the coal brick needs to be polished, and each maceral and fraction are observed and calculated correspondingly. Specific processing methods and experimental procedures refer to standard GB/T 8899-2013.[20]

2.3. Identification of the Coal Structure. *2.3.1. Macroscopic Observation of Samples.* The primary coal has the characteristics of an intact shape, a uniform and dense structure, a layered structure, and being hard. Cataclastic coal shows a secondary cataclastic structure, which also has a layered structure. Internal friction is relatively developed, especially along joint planes. The granulitic−mylonite coal was formed by serious damage to the primary coal and cataclastic coal; hence, the primary structure disappeared completely. The appearance is mostly fine-grained and fragile, with less hardness and invisible bedding.

2.3.2. Identification of Logging Curves. The stratigraphic information, such as composition and structure, could be provided by logging curves with the advantages of high sensitivity and continuity. Additionally, the evolution characteristics of strata at the time and space levels are also recorded by them. The data for the LLD, GR, DEN, and AC logging curves are obtained from multiple rounds of geological exploration in various wells in the study area. Then, the coal structure is identified by these logging curves (Table 1) and recorded according to the corresponding burial depth.

3. RESULTS AND DISCUSSION

3.1. Coal Structure Characteristics Based on Logging Curves. The resistivity, density, acoustic time difference, and diameter broadening of coal gradually decrease with a higher damage degree, and the fluctuation of logging curves is more apparent correspondingly (Figure 2). The structure of the 2# coal seam is dominated by granulitic−mylonite coal, followed by cataclastic coal and the primary coal (Tables 1 and 2), which indicates that the 2# coal seam has undergone strong tectonic deformation.

3.2. Coal Types and Different Structures of Coal. Semibright coal is the main type, followed by clarain and

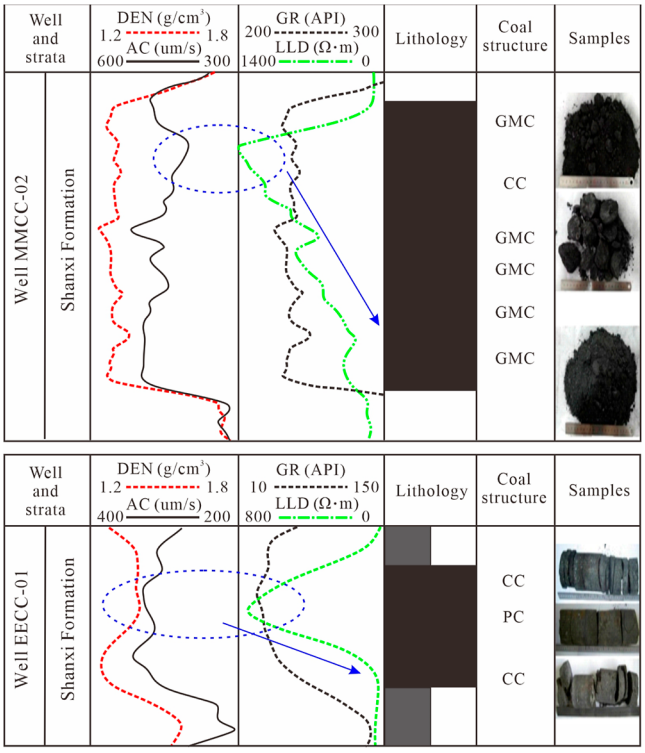

Figure 2. Logging interpretation of the coal structure based on the data of Well MMCC-02 and EECC-01. PC, CC, and GMC are primary coal, cataclastic coal, and granulitic−mylonite coal, respectively; DEN, GR, AC, and LLD are density, natural gamma ray, acoustic, and deep lateral resistivity logging curves, respectively.

Table 2. Ratios of Different Coal Structures in Different Wells

Well ID	depth (m)	thickness (m)	primary coal (%)	cataclastic coal (%)	granulitic−mylonite coal (%)
MMCC-01	1153.03	6.33	0	13.0	87.0
MMCC-02	1056.13	7.82	0	29.6	70.4
MM-91	427.49	6.1	63.8	25.5	10.6
JJLL-08	458.69	6.01	27.9	32.5	39.6
JJLL-10	461.86	5.86	10.5	38.6	50.9
WW-02	532.65	6.45	0	44.5	55.5
WW-08	583.01	6.21	34.8	43.5	21.7
ZZGG-01	686.42	6.58	100	0	0
EECC-01	777.65	7.75	62.5	12.5	25.0
EECC-02	947.69	3.9	0	100	0

Table 3. Coal Types of Different Coal Structures

type of coal structure	number of samples	fracture density(cm^{-1})	coal type
primary coal	17	2.3−7.8 5.05	semibright coal and semidull coal
cataclastic coal	14	6.7−9.1 7.9	clarain, semibright coal, semidull coal, and bleak coal
granulitic-mylonitic coal	25		clarain, semibright coal, and semidull coal

https://doi.org/10.1021/acsomega.3c04643
ACS Omega 2023, 8, 39242−39249

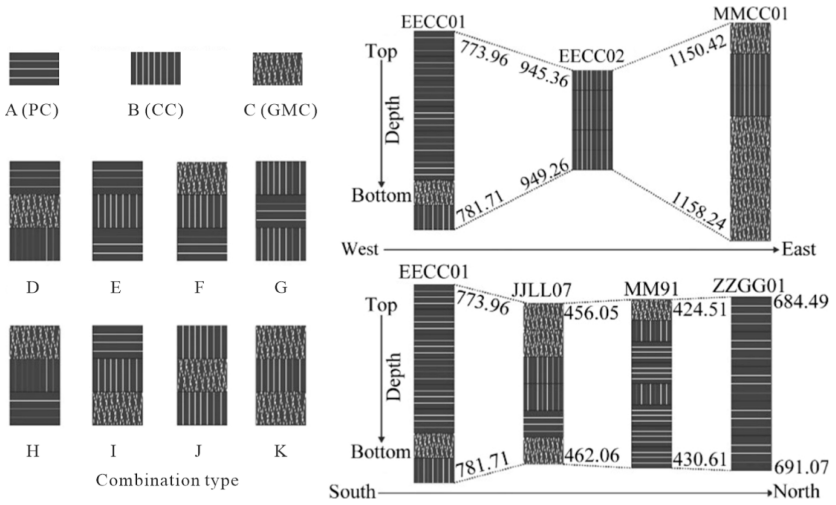

Figure 3. Vertical combination types of coal structures in the study area. PC, CC, and GMC are primary coal, cataclastic coal, and granulitic−mylonite coal, respectively.

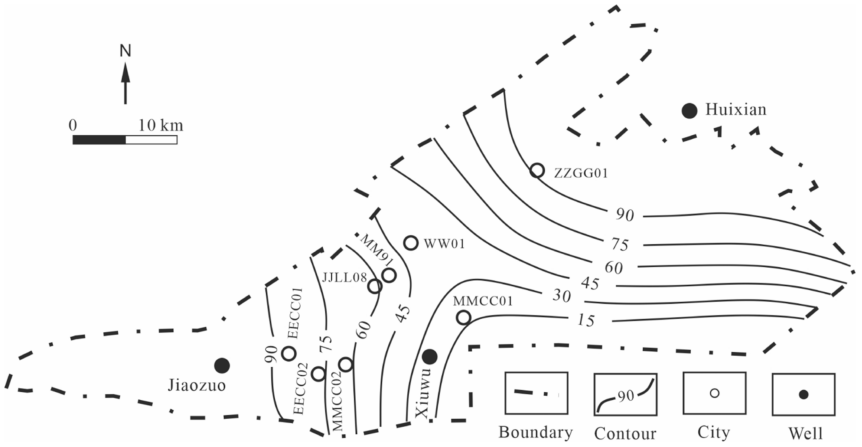

Figure 4. Contour map of the fractions of primary coal and cataclastic coal in the study area.

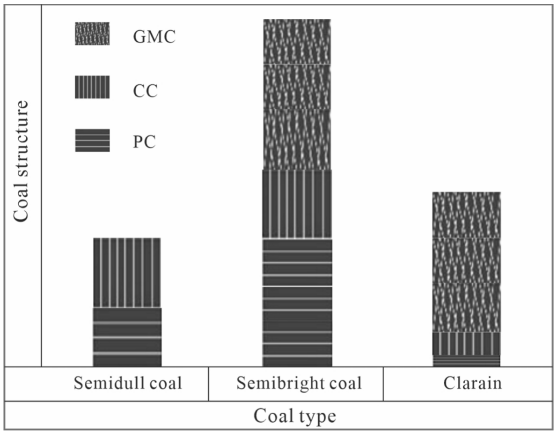

Figure 5. Relationship between coal type and coal structure. PC, CC, and GMC are primary coal, cataclastic coal, and granulitic−mylonite coal, respectively.

semidull coals (Table 3). The primary coal is mainly composed of semibright coal and semidull coal, whereas the cataclastic coal is dominated by semibright coal. The fractions of clarain and semibright coal are close in granulitic-mylonitic coal. The fracture density of primary coal is in the range of 2.3−7.8/cm (5.05/cm on average), which is lower than that of cataclastic coal (6.7−9.1/cm, 7.9/cm on average). However, the fracture density of granulitic−mylonite coal cannot be observed.

Granulitic−mylonite coal is developed in the upper and lower parts of the 2# coal seam (Figure 3). The middle part of the 2# coal seam is relatively intact and is generally composed of primary coal or cataclastic coal. The determination of the vertical combinations of coal structures is according to ref 21 Eleven types of vertical combinations are identified in this work (Figure 3), of which seven are related to granulitic−mylonite coal. Also, significant heterogeneous features are also found on the plane. From east to west of the study area, the coal structure changes from simple to complex, whereas an opposite trend is found from south to north (Figure 3). Primary coal and cataclastic coal are beneficial to coal-bed methane exploitation. Hence, it is necessary to clarify the planar characteristics of coal structures in the entire mining area. The fraction of primary coal and cataclastic coal increases from east to west and from south to north (Figure 4). In the southeast and north corners, their fractions are generally higher than 75%, and the coal structure is relatively intact (Figure 4), which can be deemed the sweet areas of coalbed methane from the perspective of the coal structure.

https://doi.org/10.1021/acsomega.3c04643
ACS Omega 2023, 8, 39242−39249

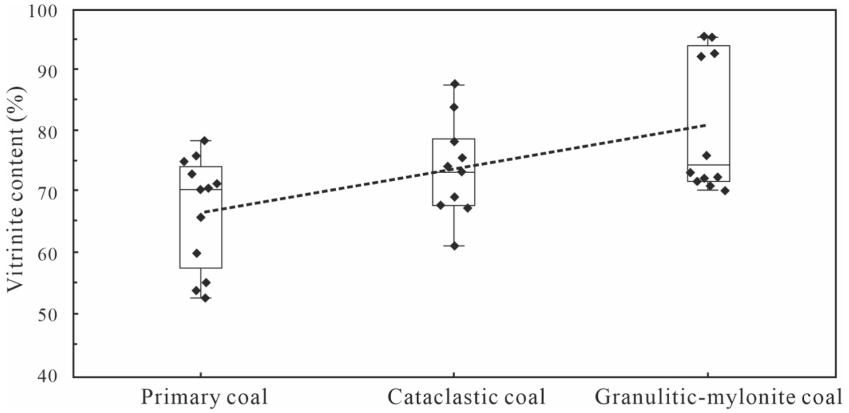

Figure 6. Vitrinite fractions in primary coal, cataclastic coal, and granulitic−mylonite coal.

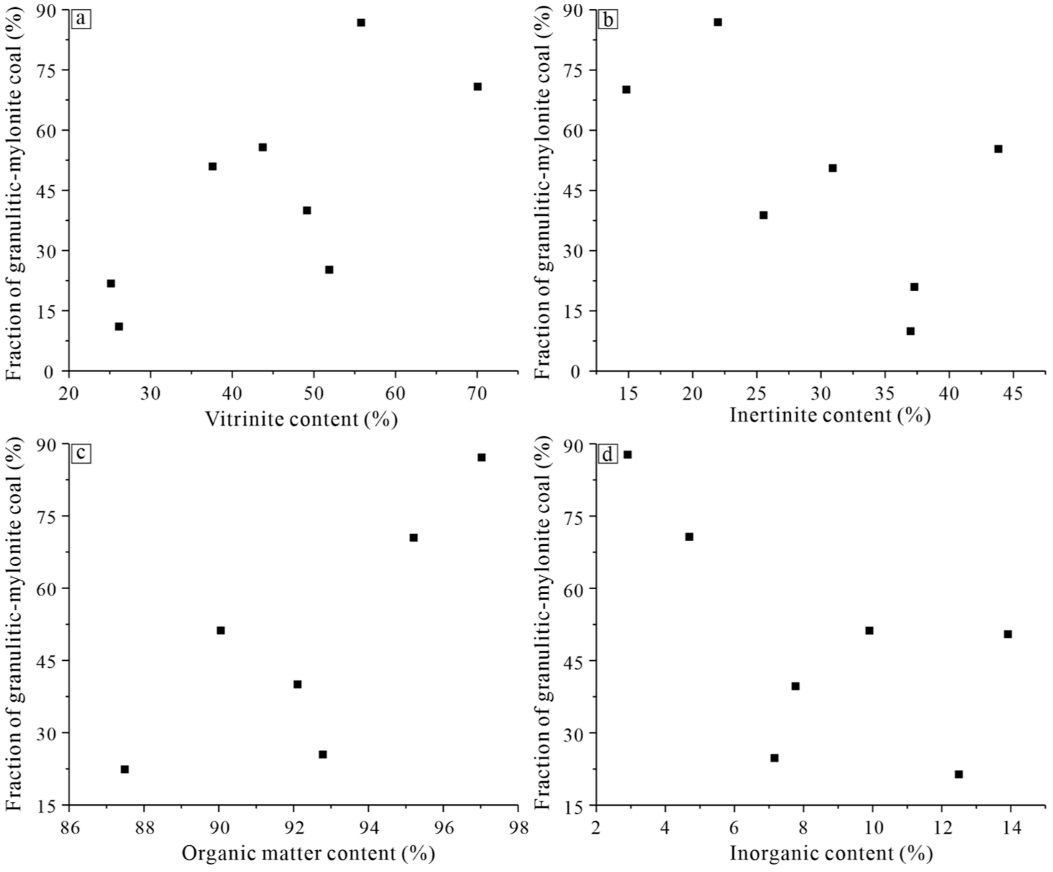

Figure 7. Relationship between the fraction of granulitic−mylonite coal and vitrinite content (a), inertinite content (b), organic matter content (c), and inorganic content (d).

3.3. Impact of Geological Properties on the Coal Structure. Primary structure and cataclastic structure are mainly developed in the semidull coal in the study area, but the granulitic−mylonite structure is not found. All three types of coal structures are recognized in the semibright coal, whereas the clarain is dominated by the granulitic−mylonite structure (Figure 5). The vitrinite content of granulitic−mylonite coal ranges from 70 to 95.14%, with an average of 81.25%, which is higher than that of cataclastic coal (61.1−87.5%, 73.59% on average) and primary coal (52.5−78.3%, 66.75% on average) (Figure 6). Furthermore, the relationship between the macerals of coal and the fractions of granulitic−mylonite coal is analyzed. The results show that the fraction of granulitic−mylonite coal roughly increases with higher vitrinite content (Figure 7a), whereas it decreases with a rise in inertinite content (Figure 7b). Additionally, coal is a type of aggregated organic matter with a content ranging from 87.52 to 97.1%, and there is a positive correlation between the fraction of granulitic−mylonite coal and the organic matter content (Figure 7c). Correspondingly, the inorganic matter content is not conducive to the development of granulitic−mylonite coal (Figure 7d).

The fraction of granulitic−mylonite coal increases with greater burial depth (Figure 8a), and a similar trend is recorded between the thickness of the coal seam and the fraction of granulitic−mylonite coal (Figure 8b). Fu et al.[22]

https://doi.org/10.1021/acsomega.3c04643
ACS Omega 2023, 8, 39242−39249

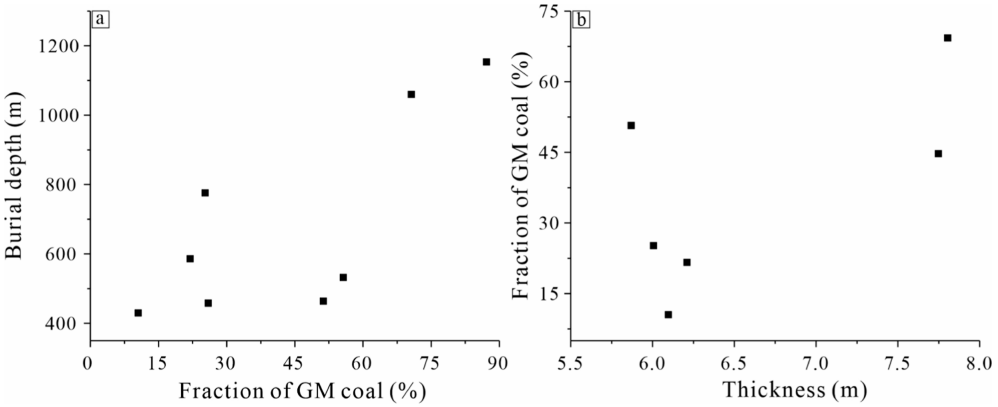

Figure 8. Relationship between the fraction of granulitic−mylonite coal and burial depth (a) and the thickness of the coal seam (b). GM is granulitic−mylonite.

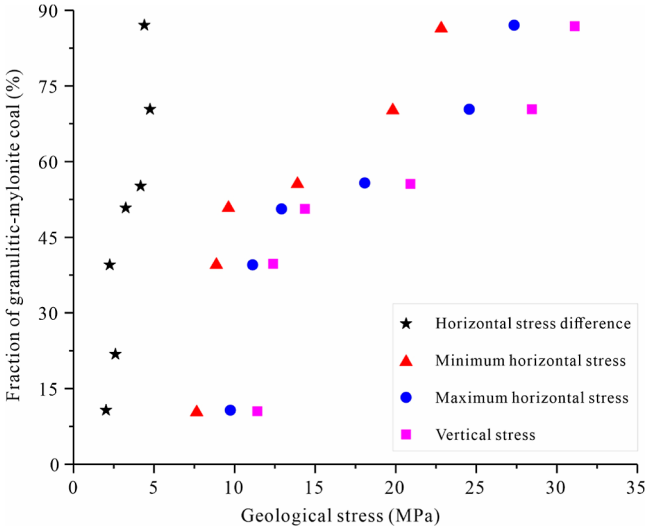

Figure 9. Relationship between the fraction of granulitic−mylonite coal and geological stress.

and Li et al.[23] also observed similar correlations, which suggests that the coal seam becomes more fragmented with greater burial depth and thickness. This is caused by changes in geological stress, and the primary coal will be damaged when the geological stress exceeds its yield limit.[24] Consequently, the relationship between geological stress (including the maximum horizontal stress, minimum horizontal stress, horizontal stress difference, and vertical stress, which are calculated using eqs 1-3[25]) and the fraction of granulitic−mylonite coal is discussed. The results exhibit that the vertical stress of the 2# coal seam ranges from 11.53 to 31.13 MPa, with an average of 20.65 MPa. The maximum horizontal stress and minimum horizontal stress are in the range of 9.78−27.34 MPa (18.09 MPa on average) and 7.72−22.87 MPa (14.71 MPa on average), respectively. The horizontal stress difference ranges from 2.06 to 4.78 MPa, with an average of 3.23 MPa (Figure 9). There are positive linear correlations between the fraction of granulitic−mylonite coal and three types of geological stress in which the regression coefficient of the maximum horizontal stress is the highest, which implies that the maximum horizontal stress is the main controlling factor of the development of granulitic−mylonite coal, although the minimum horizontal stress and vertical stress are also important reasons. Additionally, the horizontal stress difference is calculated to represent shear stress suffered by coal seams, and a positive linear correlation is recorded. The development of faults is also a significant controlling factor in the fraction of granulitic−mylonite coal. In the central part of the study area (near wells MM91, JJLL08, WW01, MMCC01, and MMCC02), large- and medium-scale faults are developed and cut into each other (Figure 1), resulting in the serious damage to the integrity of strata. Consequently, the fraction of granulitic−mylonite coal is clearly higher than that of primary coal and cataclastic coal (Figure 4). In comparison, the density of faults in the northern and western parts of the study area is relatively small and usually does not intersect with each other. Hence, primary coal and cataclastic coal are more developed.

$$S_V = \int_0^H \rho_b g \, dh \tag{1}$$

$$S_H = \left(\frac{\nu}{1-\nu} + \beta\right)(S_V - \alpha P_p) + \alpha P_p \tag{2}$$

$$S_h = \left(\frac{\nu}{1-\nu} + \gamma\right)(S_V - \alpha P_p) + \alpha P_p \tag{3}$$

S_V, S_H, and S_h are the vertical stress, maximum horizontal stress, and minimum horizontal stress, MPa; ρ_b is the coal density with different depth, g/cm^3; H is the burial depths, m; g is gravitational acceleration, m/s^2; ν is Poisson's ratio; α is the Biot coefficient; P_p is the pore pressure, MPa; β and γ are the horizontal construction coefficients.

4. CONCLUSIONS

In this work, coal samples were collected from ten wells. The coal type, coal structure, and maceral were observed and calculated, respectively. Moreover, the DEN, GR, AC, and LLD logging curves of different wells were interpreted to discuss the spatial characteristics of the coal structure. The main findings are as follows:

Granulitic−mylonite coal is the most developed in the study area, followed by primary coal and cataclastic coal. From the east to the west, the coal structure changes from simple to complex, and there is a similar trend from south to north. The coal structure is more fragmented, with greater burial depth and a larger thickness due to the change in geological stress. The proportion of granulitic−mylonite coal increases with higher geological stress. Additionally, the development of faults

https://doi.org/10.1021/acsomega.3c04643
ACS Omega 2023, 8, 39242−39249

in the central area leads to higher fractions of granulitic−mylonite coal.

■ ASSOCIATED CONTENT

Data Availability Statement

The data used to support the findings of this study are included within the article.

■ AUTHOR INFORMATION

Corresponding Authors

Jiyao Wang − *Key Laboratory of Coalbed Methane Resources and Reservoir Formation Process of the Ministry of Education, China University of Mining and Technology, Xuzhou 221116, China*; Email: jywang@cumt.edu.cn

Weidong Xie − *School of Earth Resources, China University of Geosciences, Wuhan 430074, China*; orcid.org/0000-0001-6966-6968; Email: 15262010981@163.com

Authors

Hongyue Duan − *State Key Laboratory of Intelligent Construction and Healthy Operation and Maintenance of Deep Underground Engineering, China University of Mining and Technology, Xuzhou 221008, China; Key Laboratory of Coalbed Methane Resources and Reservoir Formation Process of the Ministry of Education, China University of Mining and Technology, Xuzhou 221116, China*

Yulong Ma − *Shanxi Coal Geology Geophysical Surveying and Mapping Institute Co. LTD, Jinzhong 030600, China*

Yinlong Lu − *State Key Laboratory of Intelligent Construction and Healthy Operation and Maintenance of Deep Underground Engineering, China University of Mining and Technology, Xuzhou 221008, China*

Complete contact information is available at: https://pubs.acs.org/10.1021/acsomega.3c04643

Author Contributions

H.D., J.W., Y.L., and W.X.: Investigation, data curation, validation and writing-original draft preparation, project administration, and funding acquisition; Y.M.: methodology, conceptualization, data curation, writing-review and editing, and visualization. All authors have read and agreed to the published version of the manuscript.

Notes

The authors declare no competing financial interest.

■ ACKNOWLEDGMENTS

The authors would like to acknowledge the fund of the Major Project Cultivation of CUMT (2020-ZDPYMS09) and the Foundation Research Project of the National Science and Technology Major Project (2017ZX05035004-002).

■ REFERENCES

(1) Liu, S.; Sun, H.; Zhang, D.; Yang, K.; Li, X.; Wang, D.; Li, Y. Experimental study of effect of liquid nitrogen cold soaking on coal pore structure and fractal characteristics. *Energy* **2023**, *275*, 127470.

(2) Xie, W.; Wang, H.; Wang, M.; He, Y. Genesis, controls and risk prediction of H2S in coal mine gas. *Sci. Rep.* **2021**, *11* (1), 5712.

(3) Yu, S.; Bo, J.; Pei, S.; Jiahao, W. Matrix compression and multifractal characterization for tectonically deformed coals by Hg porosimetry. *Fuel* **2018**, *211*, 661−675.

(4) Yu, S.; Bo, J.; Jie-Gang, L. Nanopore structural characteristics and their impact on methane adsorption and diffusion in low to medium tectonically deformed coals: case study in the Huaibei coal field. *Energy Fuels* **2017**, *31* (7), 6711−6723.

(5) Hou, H.; Shao, L.; Guo, S.; Li, Z.; Zhang, Z.; Yao, M.; Zhao, S.; Yan, C. Evaluation and genetic analysis of coal structures in deep Jiaozuo Coalfield, northern China: Investigation by geophysical logging data. *Fuel* **2017**, *209*, 552−566.

(6) Zhang, S.; Men, X.; Deng, Z.; Hu, Q. Prediction Method of Coal Texture Considering Longitudinal Resolution of Logging Curves and Its Application− Taking No. 15 Coal Seam in the Shouyang Block as an Example. *ACS Omega.* **2023**, *8*, 28702−28714.

(7) Li, L.; Liu, D.; Cai, Y.; Wang, Y.; Jia, Q. Coal structure and its implications for coalbed methane exploitation: a review. *Energy Fuels* **2021**, *35* (1), 86−110.

(8) Ren, P.; Xu, H.; Tang, D.; Li, Y.; Sun, C.; Tao, S.; Li, S.; Xin, F.; Cao, L. The identification of coal texture in different rank coal reservoirs by using geophysical logging data in northwest Guizhou, China: Investigation by principal component analysis. *Fuel* **2018**, *230*, 258−265.

(9) Yang, K.; Lu, X.; Lin, Y.; Neimark, A. V. Deformation of coal induced by methane adsorption at geological conditions. *Energy Fuels* **2010**, *24* (11), 5955−5964.

(10) Li, R.; Ge, Z.; Wang, Z.; Zhou, Z.; Zhou, J.; Li, C. Effect of supercritical carbon dioxide (ScCO2) on the microstructure of bituminous coal with different moisture contents in the process of ScCO2 enhanced coalbed methane and CO2 geological sequestration. *Energy Fuels* **2022**, *36* (7), 3680−3694.

(11) Cheng, N.; Pan, J.; Shi, M.; Hou, Q.; Han, Y. Using Raman spectroscopy to evaluate coal maturity: The problem. *Fuel* **2022**, *312*, 122811.

(12) Liu, S.; Sun, H.; Zhang, D.; Yang, K.; Wang, D.; Li, X.; Long, K.; Li, Y. Nuclear magnetic resonance study on the influence of liquid nitrogen cold soaking on the pore structure of different coals. *Phys. Fluids* **2023**, *35* (1), 012009.

(13) Li, Y.; Zhang, C.; Tang, D.; Gan, Q.; Niu, X.; Wang, K.; Shen, R. Coal pore size distributions controlled by the coalification process: An experimental study of coals from the Junggar, Ordos and Qinshui basins in China. *Fuel* **2017**, *206*, 352−363.

(14) Guo, H.; Tang, H.; Wu, Y.; Wang, K.; Xu, C. Gas seepage in underground coal seams: Application of the equivalent scale of coal matrix-fracture structures in coal permeability measurements. *Fuel* **2021**, *288*, 119641.

(15) Han, Y.; Xu, R.; Hou, Q.; Wang, J.; Pan, J. Deformation mechanisms and macromolecular structure response of anthracite under different stress. *Energy Fuels* **2016**, *30* (2), 975−983.

(16) Wang, D.; Cheng, Y.; Yuan, L.; Wang, L.; Zhou, H. Experimental Study of Multiple Physical Properties of Tectonic Coal near a Minor Fault: Implications for Coal and Gas Outburst. *Energy Fuels* **2023**, *37* (8), 5878−5894.

(17) Li, X.; Zhang, X.; Shen, W.; Zeng, Q.; Chen, P.; Qin, Q.; Li, Z. Research on the mechanism and control technology of coal wall sloughing in the ultra-large mining height working face. *Int. J. Environ. Res. Public Health* **2023**, *20* (1), 868.

(18) Zhang, Z.; Ling, M.; Lin, W.; Sun, M.; Sun, W. Yanshanian Movement" induced by the westward subduction of the paleo-Pacific plate. *Solid Earth Sci. Libr.* **2020**, *5* (2), 103−114.

(19) Qin, Y.; Hou, S.; Li, D.; Zeng, J.; Cheng, G. Characteristics and Geological Significance of 2# Coal Grade Zoning in Shanxi Formation of Jiaozuo Mining Area. *Coal Geol. Explor.* **1990**, *5*, 36−39.

(20) AQSIO, SAC. *GB/T 8899-2013, Determination of maceral group composition and minerals in coal*; AQSIO, 2013;.

(21) Li, Y.; Song, Y.; Jiang, S.; Jiang, Z.; Yang, W.; Wang, Q.; Liu, D. Tight reservoir oiliness numerical simulation based on a Markov chain Monte Carlo (MCMC) method: A case study of the upper Triassic Yanchang-6 formation (T3ch6 Fm.) outcrop of Ordos Basin. *J. Pet. Sci. Eng.* **2019**, *175*, 1150−1159.

(22) Fu, X.; Qin, Y.; Wang, G. G. X.; Rudolph, V. Evaluation of coal structure and permeability with the aid of geophysical logging technology. *Fuel* **2009**, *88* (11), 2278−2285.

https://doi.org/10.1021/acsomega.3c04643
ACS Omega 2023, 8, 39242−39249

(23) Li, H.; Ogawa, Y.; Shimada, S. Mechanism of methane flow through sheared coals and its role on methane recovery☆. *Fuel* **2003**, *82* (10), 1271−1279.
(24) Li, L.; Liu, D.; Cai, Y.; Wang, Y.; Jia, Q. Coal Structure and Its Implications for Coalbed Methane Exploitation: A Review. *Energy Fuels* **2021**, *35* (1), 86−110.
(25) Huang, R. Z.; Zhuang, J. J. A new method for predicting formation fracture pressure. *Oil Drill. Prod. Technol.* **1986**, *8*, 1−14.

https://doi.org/10.1021/acsomega.3c04643
ACS Omega 2023, 8, 39242−39249